Characterization of equilibria in a low-aspect-ratio RFP

Akio SANPEI, Kensuke OKI, Ryuya IKEZOE, Takumi Onchi, Hiroyuki SHIMAZU, Tetsuo YAMASHITA, Haruhiko HIMURA and Sadao MASAMUNE

Department of Electronic Engineering, Kyoto Institute of Technology, Kyoto, 606-8585, Japan

(Received: 2 September 2008 / Accepted: 22 January 2009)

An equilibrium reconstruction code for a low-aspect-ratio reversed field pinch (RFP) plasma is developed. We reconstruct and characterize the equilibrium of the standard discharge in a low-aspect-ratio RFP device (RELAX) and estimate the bootstrap current profile on the equilibrium. Properties of estimated magnetic helicity suggest that continuous dynamo activity does exist during stable RFP configuration in RELAX.

Keywords: equilibrium reconstruction, bootstrap current, low-aspect-ratio RFP, magnetic helicity, radial transport

1. Introduction

Reversed field pinch (RFP) is one of the candidates for a high-beta, compact fusion reactor concept. Recent progress in confinement improvement has resulted in attainment of tokamak-comparable energy confinement by realizing a tearing-stable current profile with the pulsed poloidal current drive (PPCD) technique [1]. Another solution to the confinement problem may be the quasi-single helicity (QSH) RFP state, where a single dominant core-resonant tearing mode grows and closed magnetic surfaces are recovered inside the associated magnetic island [2, 3]. A scenario for steady state operation is what remains as a problem of the RFP reactor concept. Recent analysis of RFP equilibrium taking into account the neoclassical effect [4] has shown that the neoclassical bootstrap current fraction increases as the aspect ratio (A) is lowered, due mainly to an increase in neoclassical viscosity. In particular, it has been demonstrated that there exists an equilibrium with bootstrap current fraction of 94% in reactor regime plasma parameters with extremely high beta values of >60% [4].

To study these interesting characteristics of low-A RFP configurations, experiments have been carried out in RELAX (REversed field pinch of Low-Aspect ratio eXperiment) [5, 6], whose aspect ratio A=R/a=0.51m/0.25m=2, is the lowest value for RFP to date. We have developed an equilibrium reconstruction code, RELAXfit [7], by modifying the MST-Fit code [8] for low-A regimes.

2. Calculation of bootstrap current

In an equilibrium where the neoclassical effect is taken into account, the total toroidal plasma current I_ϕ^{eq} can be divided into four terms, including bootstrap current terms. I_ϕ^{eq} is expressed as

$$I_\phi^{eq} = I_\phi^{OH} + I_\phi^{PRP} + I_\phi^{BSb} + I_\phi^{BS\alpha}, \quad (1)$$

where I_ϕ^{OH} is the Ohmic current from an external electric current source, I_ϕ^{PRP} is the toroidal component of the Pfirsch-Schluter and diamagnetic currents; I_ϕ^{BSb} and $I_\phi^{BS\alpha}$ are the bootstrap currents due to the bulk plasma and fusion-produced α particles, respectively. In this code, we neglect the contribution from α particles, because RELAX is operated with only hydrogen and its plasma parameters are far from the reactor regime.

The bulk parallel bootstrap current density j^{BSb} is expressed as

$$\frac{\langle \vec{j}^{BSb} \cdot \vec{B} \rangle}{\langle \vec{B} \cdot \nabla\theta \rangle} = -\frac{p_e}{\langle 1/R^2 \rangle} \{ L_1 \left[\frac{p_e'}{p_e} + \frac{T_i}{T_e} \frac{p_i'}{p_i} / Z \right] + L_2 \frac{T_e'}{T_e} + L_3 \frac{T_i'}{T_e} / Z \} \quad (2)$$

where T and p represent the temperature and pressure, respectively, Z is the effective ionic charge, L_k (k = 1,2,3) denotes transport coefficients, θ is the poloidal coordinate, and the subscripts "e" and "i" denote electrons and ions, respectively. In our calculation, we use the transport coefficient L_k, which is a function of Z and the ratio of trapped/un-trapped particles, given by the Hirshman model [9] that assumes a plasma composed of electrons and a single ion species in the collision-less limit. j^{BSb} depends on the plasma pressure and temperature profiles. The bootstrap current increases as A decreases because the enhancement of the poloidal asymmetry due to decrease in A leads to an increase of anisotropy in the electron pressure tensor [4]. In the RFP, the toroidal component of the bootstrap current density j_ϕ^{BSb} is expected to be much smaller than in the tokamak, for example JT-60 [10], because the toroidal and poloidal components are of the same order of magnitude, and the toroidal field reverses in the plasma outer region. The RFP magnetic field configurations also affect the widths of banana orbits and neoclassical diffusion. In the RELAX parameter region, the poloidal Larmor radius of electrons $\rho_{\Omega e} \sim 4.0 \times 10^{-4}$ m is comparable

author's e-mail: sanpei@kit.ac.jp

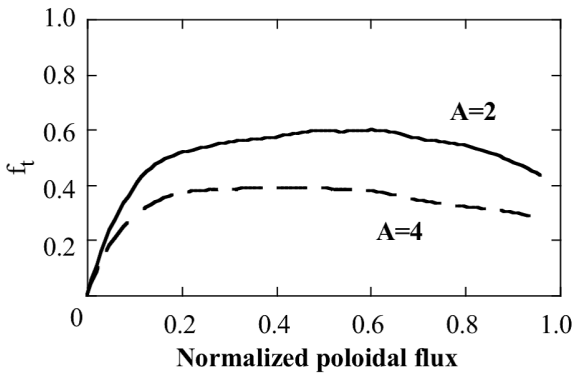

Fig. 1 Trapped fraction versus normalized poloidal flux calculated for a standard RELAX plasma. Solid line represents the trapped fraction calculated for an $A = 2$ plasma and the dashed line represents that of an $A = 4$ plasma.

with the width of the banana orbit of electron.

The ratio of trapped to untrapped particles reflects the characteristics of the equilibrium magnetic field configuration. The trapped particle fraction f_t is expressed as

$$f_t = 1 - 0.75\langle B^2\rangle \int_0^{\lambda_c} \frac{\lambda d\lambda}{\langle (1-\lambda B)^{1/2}\rangle} \qquad (3)$$

where $\lambda = \mu/E$ is the pitch angle, μ is the magnetic moment, E is energy, and the critical value $\lambda_c = 1/B_{max}$ is defined by the boundary of the loss cone. Figure 1 is a plot of the trapped particle fraction versus normalized poloidal flux $\psi_{00} = (\psi - \psi_0)/(\psi_{lim} - \psi_0)$, where ψ_{lim} is the poloidal flux at the wall, and ψ_0 is the minimum poloidal flux, i.e., $\psi_{00} = 0$ at the magnetic axis. The solid line corresponds to RELAX (A=2), while the dashed line corresponds to STE-2 (A=4), which is our old RFP machine [11], respectively. As is clear in the figure, the peak value increases up to 60% when the aspect ratio is lowered to 2, when compared with the case of A=4. The trapped particles are expected to have a strong influence in the RFP despite the small banana orbit widths, because the ratio of the bounce frequency of banana orbit ν_b to the electron-ion collision frequency ν_{ei} becomes much greater than in the tokamak. In the RELAX parameter region, $\nu_b \sim 2.0 \times 10^7$ Hz and $\nu_{ei} \sim 2.3 \times 10^5$ Hz.

3. Equilibrium in RELAX plasma

Figure 2 shows the typical time evolution of the plasma current I_p, average toroidal field $< B_\phi >$, and edge toroidal field $B_\phi(a)$. The maximum value of I_p is about 50 kA. The RFP configuration is set up in about 0.2 ms, and sustained for about 1.5 ms. A gradual increase in $< B_\phi >$ is observed during the flat-topped current phase.

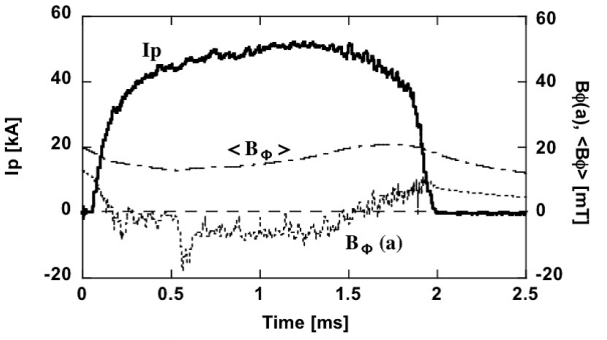

Fig. 2 Time evolution of the plasma current I_p, average toroidal field $< B_\phi >$, and edge toroidal field $B_\phi(a)$ in a typical low-A RFP discharge in RELAX.

Figure 3 shows the results of an equilibrium reconstruction of the standard RELAX discharge shown in figure 2. The magnetic field profiles are reconstructions based on experimental data at 1.5 ms. To reconstruct the equilibrium magnetic field profiles, we first specify two free functions $F = RB_\phi$ and p (plasma pressure, i.e., $p = p_e + p_i$), and then compute the resulting toroidal current density from the Grad-Shafranov equation. As experimental constrains for optimization of the reconstruction, we have used the following edge and internal magnetic diagnostic data: I_p, $< B_\phi >$, $B_\phi(a)$, the edge poloidal field $B_\theta(a)$, and radial profiles of B_ϕ and B_θ at $0.6 < r/a < 1.0$ [12] measured with an internal radial array of magnetic probes insertable from an upper port above the geometric center $R = 0.51$ m. In the optimization procedure of the most suitable reconstructed equilibrium, we set free parameters to minimize the errors of the above quantities between experimental data and estimates from the reconstructed equilibrium.

A comparison of the reconstructed equilibrium and the diagnostic data used to constrain the fit is shown in figure 3(a). The abscissa axis corresponds to the vertical line of $R = 0.51$ m. $r/a = 0$ is not the magnetic axis but the center of the poloidal cross section. The measured values of B_ϕ and B_θ are represented on the plot as cross symbols, while the fits are represented as solid and dashed lines. Note that the abscissa is the vertical coordinate in reality, although it is denoted by r/a in the figure, because it is more convenient when we compare of the reconstructed and experimental field profiles. B_θ on $r/a = 0$ is not zero, because the magnetic axis shifts approximately 0.03 m from the geometric center. This reconstruction also matches edge measurements of the total plasma current, total toroidal magnetic flux, and boundary toroidal and poloidal magnetic fields.

In this reconstruction, the plasma pressure and temperature profiles are assumed as follows: $p(\psi) = p_0(1 - \psi_{00}^3)$ and $T(\psi) = T_0(1 - \psi_{00}^3)^{0.75}$, where ψ_{00}

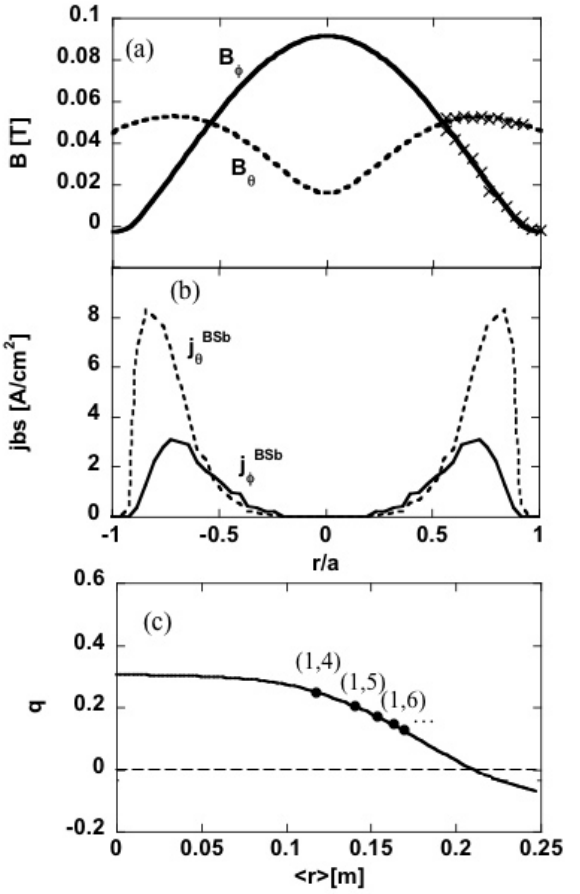

Fig. 3 (a) Reconstructed magnetic field (b) Calculated bootstrap current densities (c) Safety factor profile.

is the normalized poloidal flux, defined as $\psi_{00} = (\psi - \psi_0)/(\psi_{lim} - \psi_0)$, where ψ_{lim} is the poloidal flux at the wall, and ψ_0 is the minimum poloidal flux, i.e., $\psi_{00} = 0$ on the axis. p_0 and T_0 are the values of plasma pressure and temperatures, respectively, at the magnetic axis. The ratio of peak electron and ion pressures is set at a value typical for power balance calculations, $p_{e0}/p_{i0} = 1.07$ [13], and the ratio of temperatures is defined in a similar way.

Figure 3(b) shows the calculated toroidal j_ϕ^{BSb} (solid) and poloidal j_θ^{BSb} (dashed) bootstrap current densities. This result shows that j_ϕ^{BSb} has a hollow profile, and that j_θ^{BSb} is greater than j_ϕ^{BSb}. The hollow j_ϕ^{BSb} profile arises as follows. The bootstrap current cannot be generated on the magnetic axis because there are no trapped particles, and the trapped particle fraction is low in the vicinity of the magnetic axis, as shown in figure 1. The location of the peak of the bootstrap current strongly depends on the location of the maximum pressure and temperature gradient, and such a hollow current profile is also observed in tokamak and stellarator experiments.

In the present RELAX plasmas, the electron temperature is estimated at ~ 50 eV from soft-X ray measurements, and the density at around 10^{13} cm^{-3}. In the present case, the ratio of the toroidal bootstrap current to the toroidal equilibrium plasma current is $I_\phi^{BSb}/I_\phi^{eq} = 2.2$ kA / 50 kA $= 0.044$. The neoclassical effect does not play an important role in the present RELAX plasma parameters.

Figure 3(c) shows the radial profile of the safety factor (q). As the aspect ratio is lowered, the safety factor on axis increases and its profile becomes broader in the core region with a steeper gradient near the edge. The black points indicate the positions of the (m, n) mode rational surfaces, where $q = m/n$. In this discharge, the reconstructed q-profile implies that the innermost resonant mode is $m = 1/n = 4$, which corresponds to the experimentally observed dominant modes [14, 15].

According to RFP equilibrium analysis, the central q-value tends to increase when A is lowered. If the q on the axis is chosen so that the innermost resonance surface shifts outside, the distances between resonance surfaces extend and magnetic shear can be enlarged. The reconstructed q-profile suggests an advantage of simpler magnetic mode dynamics in low-A RFP, because mode rational surfaces are less densely spaced in the core region where overlapping of the magnetic islands tends to occur in medium- and high-aspect-ratio RFPs.

Figure 4 is another example of the equilibrium reconstruction of a RELAX plasma with a flat-topped plasma current. Figure 4 (a) shows the time evolution of the total magnetic helicity $K = \int \phi d\psi + \int \psi d\phi$ and the magnetic energy $W = \int B^2/(2\mu_0) dV$ during the flat-topped current phase. K and W are estimated after the reconstruction of the equilibria, which occurs at 0.02 or 0.03 ms each. This figure indicates that the magnetic energy tends to decay towards the end of discharge, while the total magnetic helicity is a more robust invariant. According to Taylor's relaxation theory [16], the magnetic helicity tends to decay more slowly than the magnetic energy, if there exists a resistivity anomaly caused by magnetic turbulence or large scale magnetic reconnection due to global magnetohydrodynamics (MHD) instabilities. This result suggests that some resistivity anomaly exists in the flat-topped current phase in the RELAX plasma.

Figure 4 (b) shows the radial profiles of the magnetic helicity density at 1.05 (solid line), 1.24 (light dashed line), 1.41 (heavy dashed line), and 1.56 (dotted line) ms. The positions of the maximum values of helicity density reflect the low-A equilibrium magnetic field. The time evolution of the helicity density illustrates the radially outward transport and global conservation of the magnetic helicity. These properties of K may play an important role in the self-organization of RFP plasma.

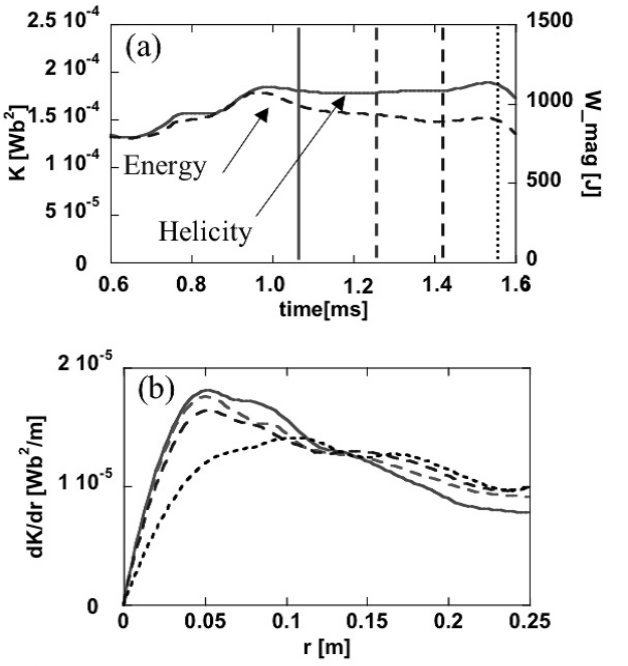

Fig. 4 (a) Time evolution of total magnetic helicity and magnetic energy. (b) Profiles of magnetic helicity.

The conservation and radial outward transport of K before and after sawtooth crush events were also estimated in Madison Symmetric Torus (MST) [8, 17]. In the MST experiments, sawtooth crush was identified as a dynamo field generation event. The dynamo effect causes helicity transport in the mean field without affecting the turbulent field. The present results of conservation and radial outward transport of K and gradual increase in $< B_\phi >$ suggest that a continuous dynamo activity does exist during the RFP configuration phase in RELAX, with redistribution of the current density profile. More detailed study of the relations between neoclassical effects and dynamo activities in low-A RFP plasmas remains as future work.

4. Summary

To analyze the characteristics of equilibrium in low-A RFP plasmas, we have developed an equilibrium reconstruction code for low-A RFP configurations including the estimation of the bootstrap current. We have demonstrated our equilibrium reconstruction of the standard discharge in a low-A RFP device, RELAX, and illustrated how the bootstrap current depends on plasma parameters. As experimental constraints for reconstruction, we used radial field profiles of B_ϕ and B_θ at $0.6 < r/a < 1.0$ measured with a radial array of magnetic probes. This code has been used successfully to estimate bootstrap current fraction in RELAX and to characterize experimental magnetic field profiles in MHD studies. In the present RELAX plasmas, the bootstrap current fraction has been estimated to be less than 5%. Radial transport and global conservation of helicity, and a tendency of the energy to decrease are observed during the RFP configuration phase.

Acknowledgments

One of the authors (A. S.) thanks Professor S. Shiina and Dr. J. Anderson for enlightening discussions. This work is supported by a U.S.-Japan collaboration and by a Grant-in-Aid for Scientific Research (No.17360441) from the Ministry of Education, Culture, Sports and Technology, and is performed with the support and under the auspices of the NIFS Collaborative Research Program (NIFS07KOAH022).

[1] J. S. Sarff *et al.*, Nucl. Fusion. **43** 1684 (2003).
[2] D. F. Escande *et al.*, Phys. Rev. Lett. **85** 1662 (2000)
[3] P. Martin *et al.*, Nucl. Fusion. **43** 1855 (2003).
[4] S. Shiina *et al.*, Phys. Plasmas. **12** 080702 (2005)
[5] S. Masamune *et al.*, *Proc. 33rd EPS Conference on Plasma Phys*, P4-136, (2006)
[6] S. Masamune *et al.*, J. Phys. Soc. Jpn. **76** (No.12), 123501 (2007)
[7] A. Sanpei *et al.*, submitted to J. Phys. Soc Jpn. (2008).
[8] J. Anderson *et al.*, Nucl. Fusion. **44** 162 (2004).
[9] S. P. Hirshman, Phys. Fluids **31** 3150 (1988).
[10] M. Kikuchi *et al.*, Nucl. Fusion. **30** 343 (1990).
[11] S. Masamune *et al.*, Fusion Energy **21** 201 (1996).
[12] K. Oki *et al.*, J. Phys. Soc. Jpn., **77**, No.7, p.075005(2008).
[13] D. A. Ehst *et al.*, Nucl. Fusion. **38** 13 (1998).
[14] T. Onchi *et al.*, Plasma Fusion Res. (RC) **3**, 005-1 - 005-2 (2008).
[15] R. Ikezoe *et al.*, Plasma Fusion Res. (RC) **3**, 029-1 - 005-3 (2008).
[16] J. B. Taylor, Phys. Rev. Lett. **33** 1139 (1974).
[17] H. Ji *et al.*, Phys. Rev. Lett. **74** 2945 (1995).